

Electronic density of states and optical spectrum of tetrahedrally bonded amorphous III-V semiconductors*

Y. F. Tsay,[†] D. K. Paul,[‡] and S. S. Mitra

Department of Electrical Engineering, University of Rhode Island, Kingston, Rhode Island 02881

(Received 17 December 1975)

The disorder in an amorphous III-V semiconductor is described in terms of spatial variation in local density. The electronic density of states for the amorphous semiconductors are then simulated by a weighted sum of the crystalline electronic density of states (EDS) with a variation in local density. It is shown that the amorphous electronic density thus obtained is equivalent to its crystalline counterpart with the energy of each electronic state broadened by an individual broadening parameter, which is related to the degree of disorder of the amorphous semiconductor considered and the "sensitivity" of the energy of the particular state to variations in local density. The result of our phenomenological model is similar to that of Kramer's complex-band-structure calculation based on Green's-function formalism. The optical spectra for the corresponding materials are also calculated using the theoretical EDS, along with the nondirect transition model with an energy-dependent matrix element. The results are compared with available experimental data.

I. INTRODUCTION

Recent investigations on the physics of amorphous materials, particularly semiconductors, have generally focused on two related questions: First, how different is the structure of an amorphous material as compared with its crystalline counterpart; and second, how are the electronic and vibrational properties of an amorphous material modified by such structural changes if the latter do exist? To find possible answers to the first question, numerous x-ray diffraction experiments¹ have been performed in order to determine the radial distribution function (RDF), which up to date provides the major experimental observable for a semiquantitative description of the structure of an amorphous semiconductor. A comparison of the amorphous and crystalline RDF's of the same tetrahedrally bonded semiconductor indicates the following:

(i) The RDF's for both the crystalline and amorphous phases are very similar, at least, up to the second-nearest-neighbor (nn) distance, implying that, at least the short-range order is preserved in the amorphous phase.

(ii) The position of the first peak of the amorphous RDF appears to shift slightly toward higher values (a few percent) as compared with those of the crystalline peak.

(iii) The first and second peaks of the amorphous RDF are fairly well defined, and are usually described, respectively, as a Gaussian of the form

$$\exp[-(r - r_{ia})^2/2\sigma_{ia}^2], \quad i = 1 \text{ or } 2, \quad (1)$$

where r_{ia} and σ_{ia} denote the position and the width, respectively.

Table I lists the relevant structural parameters of the amorphous (subscript *a*) semiconductors of interest. Corresponding crystalline (subscript *c*) values are also given for comparison. It appears that in general the width of a peak in the

TABLE I. Relevant structural parameters for amorphous III-V semiconductors.

	GaAs	GaP	GaSb	InAs
r_{1c} (Å)	2.45	2.36	2.65	2.63
r_{1a} (Å) ^a	2.48 ± 0.03	2.44 ± 0.1	2.67 ± 0.03	2.69
σ_{1c} (Å) ^a	0.085	0.015	0.079	0.075
σ_{1a} (Å) ^a	0.085 ± 0.01	0.18 ± 0.01	0.14 ± 0.01	0.09 ± 0.01
σ_1 (Å) ^b	~0.0	~0.16	~0.12	~0.05
r_{2c} (Å)	4.0	3.86	4.33	4.3
r_{2a} (Å) ^a	4.1 ± 0.05	3.9 ± 0.05	4.3 ± 0.05	4.0 ± 0.05
σ_{2c} (Å) ^a	0.109	0.1	0.105	0.114
σ_{2a} (Å) ^a	0.3 ± 0.05	0.35 ± 0.05	0.4 ± 0.05	0.3 ± 0.05
σ_2 (Å) ^b	~0.28	~0.34	~0.39	~0.28
ρ_a/ρ_c				
Calc.				
Eqs. (3) and (4)	0.92	0.90	0.81	0.77
Eq. (5) ^c	0.96	0.89	0.87	0.91
Expt. ^d	0.96	0.90	0.98	0.93
σ_p/ρ_a				
Calc.				
Eqs. (3) and (4)	0.068	0.134	0.11	0.092
Eq. (5) ^c	0.077	0.13	0.15	0.099

^a From Ref. 1.

^b Static spread in the amorphous phase obtained from Eq. (2).

^c Fitted to infrared and Raman data (see text).

^d From Ref. 16.

amorphous RDF is consistently larger than that in the crystalline phase. This is particularly true for the second peak of the RDF. The difference, which presumably may result from the structural distortions of bond lengths and/or angles, as well as wrong bond formation, is the *static* width (or spread) and is given as

$$\sigma_i^2 = \sigma_{i_a}^2 - \sigma_{i_T}^2 \approx \sigma_{i_a}^2 - \sigma_{i_c}^2, \quad i=1,2. \quad (2)$$

Here it is assumed that the thermal width σ_{i_T} of a peak in the amorphous phase is equal to the width in the crystalline phase, as the latter does not have a static width.

It must be pointed out that the RDF may not uniquely determine the microscopic structure of an amorphous material. For instance, in the case of Si and Ge, both the continuous-random-network model and the microcrystallite model² which consists of a mixture of microcrystallites with various crystalline structures, are capable of giving RDF's in close agreement with the experimental results. Although the continuous-random-network model for amorphous Si and Ge seems to be favored, it is not clear, however, that the same is true for amorphous III-V compounds.

Because of the loss of the long-range order, many theoretical works on the electronic and vibrational properties of amorphous materials have stressed the importance of the breakdown of the \vec{k} selection rule. This results in the belief that in the calculation of the electronic³ and vibrational⁴ properties of an amorphous material, use should be made of the aspects of its structure which is independent of the \vec{k} selection rules, and therefore requires an approach that is distinctly different from that used for the crystalline phase.

Recently, we have questioned the sole importance of the breakdown of the \vec{k} selection rule in explaining the basic optical properties of amorphous semiconductors. We have demonstrated⁵ that the first-order infrared and Raman spectra of a tetrahedrally bonded amorphous semiconductor (TBAS) can be interpreted as consisting primarily of a crystallinelike spectrum, whenever the optical process concerned is allowed in the crystalline phase. The residual difference is then interpreted as that arising from configurations in which only short-range order is maintained. It is our contention that the electronic structure of a TBAS can also be calculated using its crystalline analog as a starting point, but with certain modifications to take account of the structural disorders.

There are several previous calculations of the electronic structure of TBAS based on the same philosophy. Herman and Van Dyke⁶ simulated the electronic density of states (EDS) of amorphous

Ge by that of a dilated (an overall expansion of the lattice constant by 10%) Ge crystal. In order to calculate the imaginary part of the corresponding dielectric constant, they adopted the nondirect-transition model with constant matrix elements. Brust, on the other hand, calculated⁷ the ϵ_2 spectrum of a crystalline Ge with density equal to that of the amorphous phase. A substantial red shift of the spectrum was obtained, in agreement with the experimental observation.⁸ However, in order to produce the single-humped structure of the experimental ϵ_2 spectrum, a lifetime broadening of the order of 2 eV had to be used, which is about ten times as large as the crystalline value. Kramer *et al*,⁹ using the Green's-function formalism, have developed a method for calculating the electronic energy spectrum of a disordered system. By approximating the n -body spatial correlation function as products of two-body correlation functions, they obtained a complex band structure for several TBAS. The electronic energy states with the reduced wave vector \vec{k} , which in the case of crystalline solids consist of a set of δ functions, are now broadened into damped Lorentzians, the widths of which depend on \vec{k} , as well as the two-body correlation function. The latter, in turn, reflects the structural disorders in amorphous solids. According to the complex-band-structure results, the valence-band density of states (VBDS) is relatively less disturbed by disorder, and retains most of the features of its crystalline counterpart. The conduction-band density of states (CBDS), on the other hand, is profoundly changed, and is devoid of crystalline features.

In a previous paper,¹⁰ we obtained the EDS of amorphous Si and Ge by calculating the weighted average of the densities of states of the corresponding crystal with slightly different nn distances. The weighting function is taken to be a Gaussian. In the present paper, the EDS for several amorphous III-V compounds will be calculated following a similar approach. However, for reasons to become apparent below, the averaging is taken over local density distributions. The ϵ_2 spectrum will also be calculated using the EDS obtained in this paper, together with the nondirect-transition model¹¹ with energy-dependent transition-matrix elements.¹²

II. LOCAL DENSITY AND ITS DISTRIBUTION IN AN AMORPHOUS TBAS

Material inhomogeneity, voids, local strains, bond length, and bond angle variations¹³ are known to exist in most amorphous semiconductor films. As a consequence, the local density in the material is not expected to be uniform. By local density

we mean the number of atoms per unit volume averaged over a volume whose linear dimensions are of the order of several multiples of the bond length. As mentioned above, the static spread in the first and second peak of the RDF of a TBAS may by themselves result in a spatial fluctuation of the local density. A quantitative analysis of the spatial variation of local density, including inhomogeneity, void structure, local strains, as well as bond length and angle distortions, is a formidable task. However, if one assumes that the local density variation results principally from the spreads of the first and second nn distances then a distribution in local density can be estimated, in the following way: First, a reasonable definition¹⁴ for local density in terms of the first and the second nn distances r_1 and r_2 is made

$$\rho(r_1, r_2) = 3\left(\frac{3}{8}\right)^{1/2} \left(\frac{1}{r_1^3} + C \frac{K^3 - 1}{r_2^3 - r_1^3} \right) / (1 + C), \quad (3)$$

where $K = r_{2a}/r_{1a}$ and C is a weighting factor determining the relative importance of the second nn's in contributing to the local density. The rationale for such a definition is discussed in detail else-

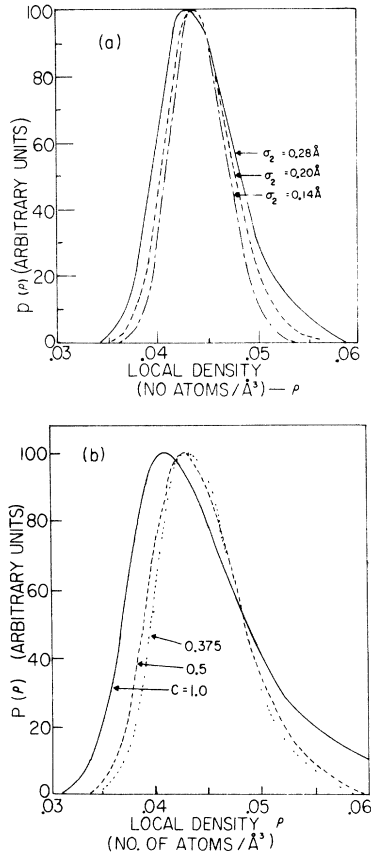


FIG. 1. (a) Distribution of local density for various values of σ_2 (see text). (b) Distribution of local density for various values of C (see text).

where.¹⁴ In order to calculate the distribution of the local density, a deviation of $r_1(r_2)$ by about $\sigma_1(\sigma_2)$ from its mean value $r_{1a}(r_{2a})$ is considered. If it is assumed that for these ranges of r_1 and r_2 , their respective probability distributions are independent, then their joint probability distribution is given by

$$P(r_1, r_2) \propto \exp \left\{ -0.5 \left[\left(\frac{r_1 - r_{1a}}{\sigma_1} \right)^2 + \left(\frac{r_2 - r_{2a}}{\sigma_2} \right)^2 \right] \right\}. \quad (4)$$

In Eq. (4), σ_1 and σ_2 are, respectively, the *static* spread of the first and the second peaks in the amorphous RDF, as given in Table I. From Eqs. (3) and (4), the local density distribution can be calculated. Figure 1 shows the general shape of the local density distribution of amorphous Ge, and its dependence on σ_2 and C , respectively. Results for III-V compounds are similar. It is seen that, except for a slight asymmetry, the local density distribution is approximately Gaussian. We point out, however, that the approach outlined above should be regarded as only a preliminary attempt to calculate the local density distribution. It is believed, however, that although the peak position and width may not be accurately predicted, as there is no physical guidance to fix the value of C , the general shape of the local density distribution may be correct. Therefore, before a better method for calculating the local density distribution, including bond and dihedral angles, becomes available, one may for practical purposes, take it as a Gaussian of the following form:

$$P(\rho) = \exp[-(\rho - \rho_a)^2 / 2\sigma_\rho^2], \quad (5)$$

with the mean ρ_a and the variance σ_ρ as adjustable parameters.

In this work ρ_a and σ_ρ have been obtained in two different ways. First, $P(\rho)$ is determined from Eqs. (3) and (4) with $C = 0.375$. Second, these two quantities are used as adjustable parameters in Eq. (5) in fitting¹⁵ the main features of infrared and/or Raman spectra of TBAS.⁵ The values of ρ_a and σ_ρ obtained by these two methods along with the experimental values¹⁶ of ρ_a are compared in Table I. In general the agreement is remarkably good.

III. CALCULATION OF ELECTRONIC DENSITY OF STATES

In analogy with the point of view adopted for interpreting the lattice spectra of a TBAS, as discussed in the last section, we make the following assumption:

$$N_a(E) \approx \int N_c(E, \rho) \exp\left(-\frac{(\rho - \rho_a)^2}{2\sigma_\rho^2}\right) d\rho, \quad (6)$$

where $N_a(E)$ stands for the electronic density of

states at energy E of a TBAS. $N_c(E, \rho)$ is the corresponding crystalline density of states for the local density ρ . The above assumption amounts to neglecting the contribution arising from highly disordered structural configurations. Next, if $N_c(E, \rho)$ is written

$$N_c(E, \rho) = \sum_n \sum_k \delta(E - E_{n,k}(\rho)), \quad (7)$$

then

$$N_a(E) \approx \sum_n \sum_k \int \delta(E - E_{n,k}(\rho)) \times \exp\left(-\frac{(\rho - \rho_a)^2}{2\sigma_\rho^2}\right) d\rho. \quad (8)$$

In Eqs. (7) and (8), the subscript k should not be regarded as carrying the usual meaning of wave vector, which is a good quantum number for an electronic state in a perfect crystal. Instead, it is just an index by which electronic states are enumerated.

In general, we expect the local density distribution to be sharply peaked around its mean value ρ_a . Therefore, most contribution to the integral in Eq. (8) comes from ρ , for which $|\rho - \rho_a| \sim \sigma_\rho \ll \rho_a$; in this range of ρ , $E_{n,k}(\rho)$ can be expanded as

$$E_{n,k}(\rho) = E_{n,k}(\rho_a) + \gamma_{n,k}(\rho - \rho_a) + \dots, \quad (9)$$

where

$$\gamma_{n,k} \equiv \left. \frac{\partial [E_{n,k}(\rho)]}{\partial \rho} \right|_{\rho = \rho_a}. \quad (10)$$

Equation (8) can then be rewritten

$$N_a(E) \propto \sum_{n,k} \frac{1}{\gamma_{n,k}} \exp\left(-\frac{[E - E_{n,k}(\rho_a)]^2}{2\sigma_{n,k}^2}\right), \quad (11)$$

where

$$\sigma_{n,k} \equiv \gamma_{n,k} \sigma_\rho. \quad (12)$$

It is seen therefore, that the δ functions in Eq. (7) for the crystalline phase are now replaced by a series of Gaussians. The width of the Gaussian is given by $\sigma_{n,k}$, which is the product of the density spread parameter σ_ρ , and $\gamma_{n,k}$, the derivative of the electronic energy $E_{n,k}$ with respect to the local density.

To calculate $\gamma_{n,k}$ use can be made of the following equation:

$$\gamma_{n,k} \equiv \left. \frac{\partial E_{n,k}}{\partial \rho} \right|_{\rho = \rho_a} = \frac{1}{\rho_a K} \left. \frac{\partial E_{n,k}}{\partial P} \right|_{P = P_a}, \quad (13)$$

provided the pressure (P) coefficient of $E_{n,k}$ is known. In Eq. (13), K is the isothermal compressibility. The problem then reduces to finding $\partial E_{n,k}/\partial P$. This latter quantity can, in principle,

be estimated from high-pressure data. Unfortunately, most experimental data are related to the pressure coefficients of a few optical transitions, which actually consists of the relative pressure induced shifts of the energy levels of the initial and final states. We therefore resort to a pressure-dependent band-structure calculation.¹⁷ Specifically, the calculation uses only the compressibility and the empirical pseudopotential form factors appropriate for describing the crystalline band structure at normal pressure as input data. The predicted pressure coefficients at several critical-point band gaps are in good agreement with the available experimental data in the cases of elemental and III-V compound semiconductors. In the above-mentioned calculation, it is assumed, as in most previous calculations,¹⁸ that the energy of the top valence states (Γ_{15} in the zinc-blende-type, and Γ_{25} in the diamond-type crystals) does not change with pressure, since it is only the relative shifts of the initial and final states defining the band gap (optical transition) that are of interest. We believe that such a method is also adequate for estimating the pressure shift of $E_{n,k}$'s, provided that the pressure coefficient of the energy, $E(\Gamma_{15})$, of the top valence states is known. The pressure coefficient $dE(\Gamma_{15})/dP$, in fact, can be obtained from the appropriate volume deformation potential, which occurs in the theory of electron-phonon interaction. Unfortunately, experimental values of $dE(\Gamma_{15})/dP$ are scarce and somewhat controversial. For example, Herring and Vogt¹⁹ gave a value of -3.6×10^{-6} eV/bar for Ge, based on transport properties of the crystal. Whereas Bagguley *et al.*²⁰ from cyclotron resonance measurement, estimated the value to be $\sim +4 \times 10^{-6}$ eV/bar, which agrees, in sign, with the theoretical prediction of Kleinman²¹ for Si. To our knowledge, no appropriate values exist for III-V semiconductors. In the present work, we shall assume that the shift of the topmost valence state with pressure is negligible, i.e., $dE(\Gamma_{15})/dP \approx 0$. The final results of the calculation, however, do not depend sensitively on the exact value of $dE(\Gamma_{15})/dP$, as long as its absolute value remains small, which seems to be the case.

In actual calculation, whenever available, use has been made of the modified pseudopotential form factors due to Chelikowsky *et al.*,²² which agree well with the energy of the low-lying valence bands recently determined from x-ray photoemission data.^{23,24} The effect of mean-density deficiency in the amorphous state as compared with its crystalline counterpart is accounted for in an approximate way by scaling the pseudopotential form factors according to density, as was previously done by Brust.⁷

To obtain the EDS, we calculate $E_{n,k}(\rho_0)$ and $\gamma_{n,k}$ at 1500 different \vec{k} values in the Brillouin zone. A linear interpolation is then used to sample a finer \vec{k} mesh of about a quarter million points in order to suppress the statistical "noise" in the histogram. The sampling procedure is capable of generating the crystalline EDS in excellent agreement in details of fine spectral features with those obtained recently by Chelikowsky *et al.*²²

The imaginary part of the dielectric constant $\epsilon_2(\omega)$ in the one-electron approximation may be written

$$\epsilon_{2,a} \sim (1/\omega^2) |M(\omega)|_a^2 N_{\text{conv}}(\omega), \quad (14)$$

where $|M(\omega)|_a^2$ is the amorphous matrix element and $N_{\text{conv}}(\omega)$ is the convoluted densities of states of the valence and conduction bands for which energy is conserved. $|M(\omega)|_a^2$ is obtained from that of the crystalline phase by smoothing the unklapp peak,²⁵ which often originates from long-range order.

IV. RESULTS AND DISCUSSIONS

Figure 2(a) shows the crystalline $E-\vec{k}$ diagram (full line) along the [100] and [111] directions. The bars indicate the relative magnitude of $\gamma_{n,k}$. GaP is taken as an illustrative example. Results for other materials considered in this paper are similar. It is observed that the conduction states, in general, have larger $\gamma_{n,k}$ than the valence states. This, of course, is expected because the conduc-

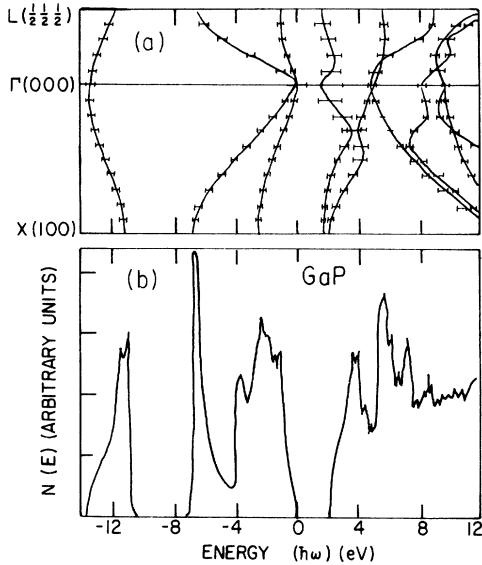


FIG. 2. (a) $E-\vec{k}$ diagram of crystalline GaP along the [100] and [111] directions. The vertical bars indicate the relative magnitude of $\gamma_{n,k}$. (b) Electronic density of states of crystalline GaP.

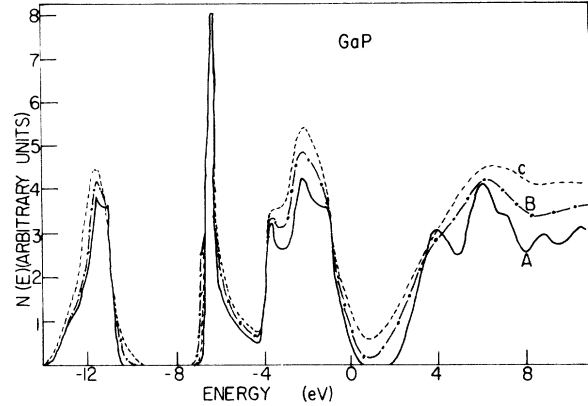


FIG. 3. Calculated electronic density of states of amorphous GaP with various values of disorder parameter, σ_ρ/ρ_a . Curve A: $\sigma_\rho/\rho_a = 0.05$; curve B: $\sigma_\rho/\rho_a = 0.13$; curve C: $\sigma_\rho/\rho_a = 0.20$.

tion-band wave functions are extended in space and therefore are more sensitive to the change of the local atomic volume due to the local density fluctuation. The calculated crystalline density of

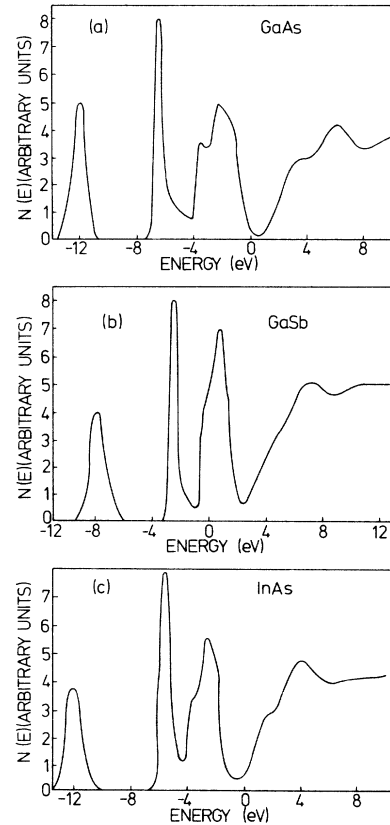


FIG. 4. Calculated electronic density of states for amorphous GaAs, GaSb, and InAs. σ_ρ/ρ_a values used for these curves are those obtained from the fitting of first-order infrared and Raman spectra (see Table I).

states for GaP is shown in Fig. 2(b).

Figure 3 shows the calculated EDS for GaP with various values of the "disorder parameter" σ_p/ρ_a . Curve A of Fig. 3 is the least disordered. The VBDS is essentially the same as its crystalline counterpart except for some smoothing out of the fine structures in the upper-most valence band. The CBDS, on the other hand, has already shown substantial departure from the crystalline density of states although the broad profiles remain. For curves B and C, the values of σ_p/ρ_a are 0.13 and 0.20, respectively. The changes in the VBDS and CBDS with the degree of disorder are clearly shown by the trend manifested by these curves. Several points are particularly worth mentioning: (i) the widths of peaks of the VBDS are very little affected by disorder except for the tailing of density of states into the crystalline gaps; (ii) higher

degrees of disorder produce larger tailings. This is particularly significant regarding the crystalline optical gap, as is vividly shown in Fig. 3; (iii) for higher degrees of disorder, e.g., curves B and C in Fig. 3, the structures in the crystalline density of states have all but disappeared, and in its place, is a single hump followed by a flat plateau. Similar single-hump CBDS has recently been reported by Eastman *et al.*²⁶ for amorphous Ge, which is significantly different from the totally flat CBDS previously deduced by Donovan *et al.*²⁷ from ultraviolet photoemission data. Although no experimental data on the CBDS of III-V amorphous semiconductors are available at the present, such a one-hump structure for amorphous III-V compounds is highly possible, because of the similarity of their electronic structures to that of Ge. Figure 4 shows the EDS for the other amorphous solids

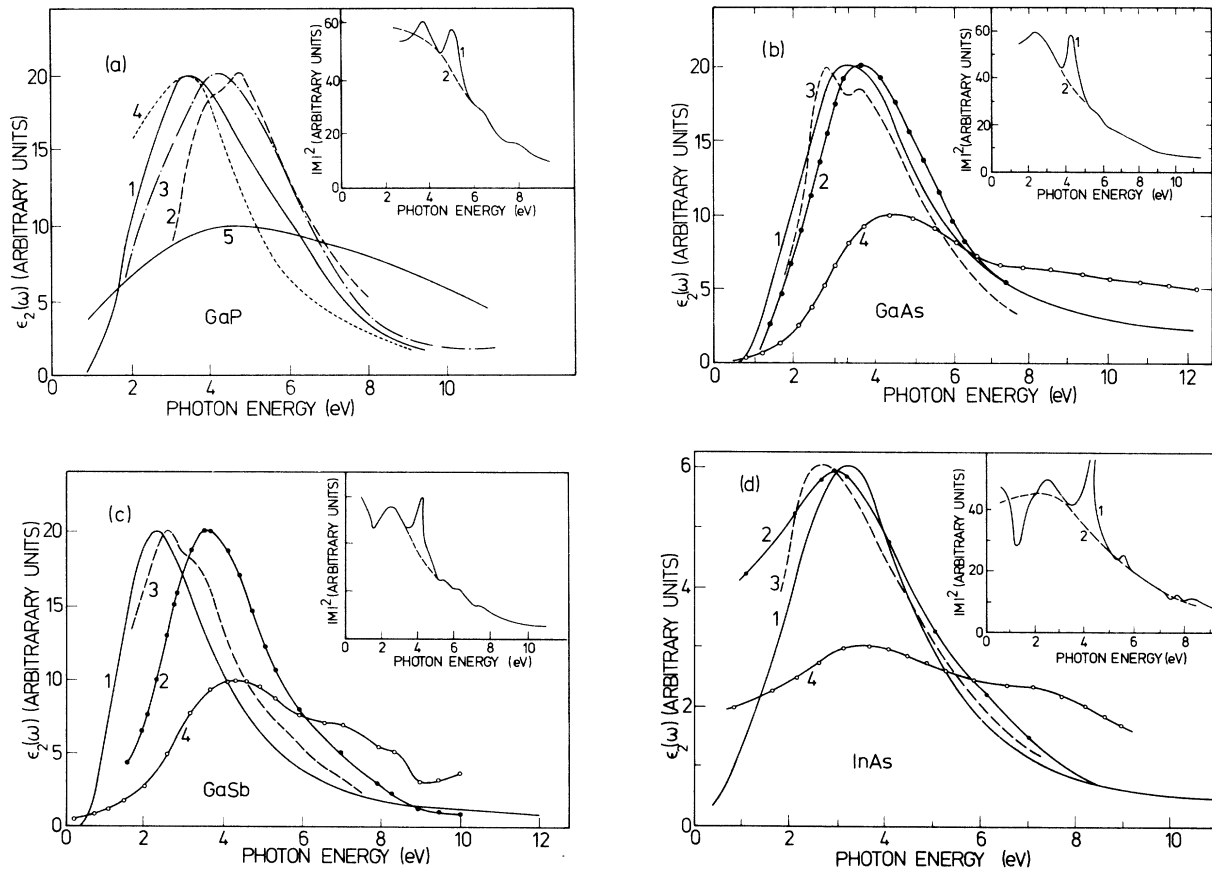


FIG. 5. Imaginary part of the dielectric constant versus photon energy for amorphous III-V compounds. (a) GaP: Curve 1—experimental (Ref. 16); curve 2—calculated by Kramer *et al.* (Ref. 9); curve 3—calculated in this paper using EDS with $\sigma_p/\rho_a = 0.13$; curve 4—calculated in this paper using EDS with $\sigma_p/\rho_a = 0.20$; curve 5—calculated using EDS with $\sigma_p/\rho_a = 0.13$ and with constant matrix element. (b) GaAs: Curve 1—experimental (Ref. 16); curve 2—calculated in this paper using the EDS of Fig. 4; curve 3—calculated by Kramer *et al.* (Ref. 9); curve 4—the same as curve 2 except for the use of constant matrix element. (c) GaSb: for legends, see (b). (d) InAs: for legends, see (b). Inserts to (a)–(d): curve 1—crystalline $|M(\omega)|^2$; curve 2—amorphous $|M(\omega)|^2$ used in the present calculation.

considered in the present paper. In all cases, the changes due to disorder in the VBDS are much less significant as compared with the corresponding changes in the CBDS. The VBDS for several crystalline^{23,24} and amorphous²³ III-V and II-VI semiconductors have been determined by Shevchik *et al.* from x-ray photoemission experiment. They concluded that the VBDS of an amorphous compound is essentially a broadened version of its crystalline counterpart. The results of the present calculation indicate the same, although the extent of broadening is not significant except in the tailing parts of VBDS. However, we would like to point out that in the experimental results of Shevchik *et al.*, the crystalline VBDS themselves are also greatly broadened when compared with theoretically calculated VBDS. We feel that since the amorphous VBDS are determined by the same experimental setup, a significant part of their broadening might have the same origin as their crystal counterpart and therefore does not result from the effects of disorder.

The imaginary part of the dielectric constant $\epsilon_2(\omega)$ for the amorphous III-V compounds as obtained from the present calculated density of states are compared in Figs. 5(a)–5(d) with those of Kramer *et al.*⁹ and experimental data.¹⁶ The energy dependence of the matrix elements [shown as inserts in Figs. 5(a)–5(d)] gives better agreement. The agreement between the calculated and experimental $\epsilon_2(\omega)$ is quite good for GaAs, GaP, and InAs. For GaSb, the calculated result is less satisfactory, in that the predicted peak position of $\epsilon_2(\omega)$ is shifted from that of experimental data by more than 1 eV. The shape of $\epsilon_2(\omega)$ curve, however, is fairly well predicted. Presumably the calculated peak position can be shifted to coincide with the experimental one by using a different energy-dependent matrix element or by using a significantly different value of ρ_a , which would reduce the “pseudo”-optical band gap, so as to cause stronger absorption at lower energies, i.e., a red shift of the absorption peak to lower energies.

*Supported in part by Air Force Cambridge Research Laboratories (AFSC), Contract Nos. F19628-72-C-0286 and F19628-75-C-0163.

†Present address: NRC Postdoctoral Resident Research Associate at Solid State Sciences Division, RADC/ETSS, Hanscom AFB, Ma. 01731.

‡Present address: Dept. Electrical Engineering, Indian Institute of Technology, Kanpur (U.P.), India.

¹See, for example, N. J. Shevchik and W. Paul, *J. Non-Cryst. Solids* **13**, 1 (1974), and references therein.

²G. P. Betteridge, *J. Phys. C* **6**, L427 (1973).

³See, for example, D. Weaire and M. Thorpe, *Phys. Rev. B* **4**, 2508 (1971); M. F. Thorpe and D. Weaire, *ibid.* **4**, 3518 (1971); B. Y. Tong, *AIP Conf. Proc.* **20**, 145 (1974).

⁴See, for example, R. Alben, *AIP Conf. Proc.* **20**, 249 (1974).

⁵S. S. Mitra, D. K. Paul, Y. F. Tsay, and B. Bendow, *AIP Conf. Proc.* **20**, 284 (1974); *Phys. Status Solidi B* **72**, 475 (1975); *Proceedings of the Third International Conference on Light Scattering in Solids*, edited by M. Balkanski, R. C. Leite, and S. P. S. Porto (Flammarion, Paris, 1976), p. 646.

⁶F. Herman and J. P. Van Dyke, *Phys. Rev. Lett.* **21**, 1575 (1968).

⁷D. Brust, *Phys. Rev.* **186**, 768 (1969); and *Phys. Rev. Lett.* **23**, 1232 (1969).

⁸T. M. Donovan, W. E. Spicer, and J. M. Bennett, *Phys. Rev. Lett.* **22**, 1058 (1969).

⁹B. Kramer, K. Maschke, and P. Thomas, *Phys. Status Solidi B* **48**, 635 (1971).

¹⁰Y. F. Tsay, D. K. Paul, and S. S. Mitra, *Phys. Rev. B* **8**, 2827 (1973).

¹¹J. Tauc, *Mater. Res. Bull.* **3**, 37 (1968); also in *Optical*

Properties of Solids, edited by S. Nudelman and S. S. Mitra (Plenum, New York, 1969), p. 123.

¹²K. Maschke and P. Thomas, *Phys. Status Solidi* **41**, 743 (1970).

¹³See, for example, N. J. Shevchik and W. Paul, *J. of Non-Cryst. Solids* **16**, 55 (1974).

¹⁴J. F. Vetelino and S. S. Mitra, in *Physics of Structurally Disordered Solids*, edited by S. S. Mitra (Plenum, New York, 1976), p. 541.

¹⁵Y. F. Tsay, B. Bendow, and S. S. Mitra, *J. Electron. Mater.* **5**, 995 (1975).

¹⁶J. Stuke and G. Zimmerer, *Phys. Status Solidi B* **49**, 513 (1972).

¹⁷Y. F. Tsay, S. S. Mitra, and B. Bendow, *Phys. Rev. B* **10**, 1476 (1974).

¹⁸See references cited in Ref. 17.

¹⁹C. Herring and E. Vogt, *Phys. Rev.* **101**, 941 (1956).

²⁰D. M. S. Bagguley, D. W. Flaxen, and R. A. Stradling, *Phys. Rev. Lett.* **1**, 111 (1962).

²¹L. Kleinman, *Phys. Rev.* **130**, 2283 (1963).

²²J. Chelikowsky, D. J. Chadi, and M. L. Cohen, *Phys. Rev. B* **8**, 2786 (1973).

²³N. J. Shevchik, J. Tejada, and M. Cardona, *Phys. Rev. B* **9**, 2627 (1974).

²⁴D. E. Eastman, W. D. Grobman, J. L. Freeouf, and M. Erbudak, *Phys. Rev. B* **9**, 3473 (1974).

²⁵J. C. Phillips, *Solid State Physics*, edited by H. Ehrenreich, F. Seitz, and D. Turnbull (Academic, New York, 1966), Vol. 18, p. 55.

²⁶D. E. Eastman, J. L. Freeouf, and M. Erbudak, *AIP Conf. Proc.* **20**, 95 (1974).

²⁷T. M. Donovan and W. E. Spicer, *Phys. Rev. Lett.* **21**, 1572 (1968); *Phys. Rev. B* **2**, 397 (1970).